

Silicon Carbide Based Nanotubes as a Sensing Material for Gaseous H_2SiCl_2

Doust Mohammadi, Mohsen; Abdullah, Hewa Y.; Bhowmick, Somnath; Biskos, George

DOI

[10.1007/s12633-022-02010-0](https://doi.org/10.1007/s12633-022-02010-0)

Publication date

2022

Document Version

Final published version

Published in

Silicon

Citation (APA)

Doust Mohammadi, M., Abdullah, H. Y., Bhowmick, S., & Biskos, G. (2022). Silicon Carbide Based Nanotubes as a Sensing Material for Gaseous H_2SiCl_2 . *Silicon*, 15(1), 177-186. <https://doi.org/10.1007/s12633-022-02010-0>

Important note

To cite this publication, please use the final published version (if applicable). Please check the document version above.

Copyright

Other than for strictly personal use, it is not permitted to download, forward or distribute the text or part of it, without the consent of the author(s) and/or copyright holder(s), unless the work is under an open content license such as Creative Commons.

Takedown policy

Please contact us and provide details if you believe this document breaches copyrights. We will remove access to the work immediately and investigate your claim.

Green Open Access added to TU Delft Institutional Repository

'You share, we take care!' - Taverne project

<https://www.openaccess.nl/en/you-share-we-take-care>

Otherwise as indicated in the copyright section: the publisher is the copyright holder of this work and the author uses the Dutch legislation to make this work public.



Silicon Carbide Based Nanotubes as a Sensing Material for Gaseous H_2SiCl_2

Mohsen Doust Mohammadi¹ · Hewa Y. Abdullah² · Somnath Bhowmick³ · George Biskos^{3,4}

Received: 5 May 2022 / Accepted: 1 July 2022 / Published online: 14 July 2022
© The Author(s), under exclusive licence to Springer Nature B.V. 2022

Abstract

The ability of carbon- and silicon-based nanotubes, including pure carbon, silicon carbide, and Ge-doped silicon carbide nanotubes (CNT, SiCNT, SiCGeNT, respectively), for sensing highly toxic dichlorosilane (H_2SiCl_2) are investigated using quantum chemistry calculations. The intermolecular interactions between the sensing material and the gas molecule have been investigated with the density functional theory calculations with a functional that includes dispersion terms. The selected method employed is B3LYP-D3 (GD3BJ)/6-311G(d), while other functionals including PBE0, ω B97XD, and M06-2X have been used for comparison. The quantum theory of atoms in molecules (QTAIM) analysis is employed to check the type of intermolecular interactions. Natural bond orbital (NBO) calculations have been used to deduce the bond orders. The findings of this work indicate that the adsorption of the H_2SiCl_2 is a physisorption process, which is very desirable for its function as a sensing element. The Ge-doped nanotube offers maximum adsorption energy in comparison to CNT and SiCNT.

Keywords Carbon nanotube · DFT · Dichlorosilane · Silicon carbide · Wave function analysis

1 Introduction

Developing materials for a gas sensor is of paramount importance for a number of applications, including for health and safety at the workplace [1]. For example, having gas sensors that can detect and measure the concentrations of dichlorosilane (H_2SiCl_2) during the manufacturing of semiconducting silicon wafers is of crucial importance for the protection of workers in the silicon industry [2]. To this end, identifying elements that can make the sensing materials more sensitive, selective and able to respond fast to changes in the target gas is an ever-ending requirement. What is more, being able to synthesize these materials in

an easy and cost-effective way can provide an important advantage for their widespread use.

Nanomaterials are formed in a variety of morphologies, and ironically many of these nanostructures provide suitable substrates for reaction with other materials. The most famous forms of nanomaterials are nanotubes [3], nanosheets [4, 5], and nanocages, which have been extensively studied theoretically in the form of quantum chemistry and solid-state physics and other related disciplines. One of the most efficient structures in nanotechnology has been the use of nanotubes consisting of carbon or a combination of carbon and silicon, which has been used extensively in drug delivery, electronic devices, and so on. The remarkable properties of these nanotubes have been studied in many previous studies [6].

Highly toxic, corrosive, and flammable gas dichlorosilane (H_2SiCl_2), DCS, is widely used in the silicon-based semiconductor industry. Therefore, in such industries, high doses of such lethal gas are harmful to the environment and human health and must be controlled [7]. Thus, the design of sensors sensitive to this gas is of particular importance. The method of synthesis of DCS is mentioned in many sources and has a long history [8]. Due to its widespread use in industry, H_2SiCl_2 has received much attention and quantum calculations to fully understand its hydrolysis have been studied at the G2 level

✉ Hewa Y. Abdullah
hewayaseen@gmail.com

¹ School of Chemistry, College of Science, University of Tehran, Tehran 14176, Iran

² Physics Education Department, Faculty of Education, Tishk International University, 44002 Erbil, Kurdistan Region, Iraq

³ Climate and Atmosphere Research Centre, The Cyprus Institute, 2121 Nicosia, Cyprus

⁴ Faculty of Civil Engineering and Geosciences, Delft University of Technology, Delft 2628 CN, The Netherlands

[9]. In addition, intermolecular interactions of this gas with specific nanostructures have been theoretically investigated by our research group [10, 11].

Here we examine the adsorption of DCS on the surface of pristine carbon nanotube (CNT), silicon carbide as well as Ge-doped silicon carbide nanotubes (SiCNT and SiCGeNT, respectively). The rest of the paper is organised as follows. Section 2 provides brief background information for the quantum computations used in this study. Section 3 describes how the geometric optimization calculations were carried out, lists the Conceptual DFT cases, and discusses the results of natural bond orbital (NBO) and quantum theory of atoms in molecules (QTAIM) analyses are given, respectively. Finally, Sect. 4 summarizes the most important conclusions.

2 Computational Details

The *ab initio* calculations carried out in this study are at the density functional theory (DFT) level. The B3LYP-D3 (GD3BJ) functional in combination with the 6-311G(d) basis set has been employed in all calculations, including optimization of structures as well as wave function analysis. Grimme's D3 dispersion correction with Becke-Johnson damping together with B3LYP functional has shown to be an effective model to describe intermolecular forces [12]. On the other hand, the data obtained from previous benchmark calculations indicate good accuracy of the chosen basis set [13–17].

Other functionals, such as PBE0 [18, 19], M06-2X [20, 21], and ω B97XD, have also been used for geometry optimization and, consequently, for comparison with B3LYP-D3 (GD3BJ) functional. We have used Gaussian 16 Rev. C.01 [22] package for electronic structure calculations. A very tight convergence criterion (1.5×10^{-5} Hartree) has been implemented for all calculations. In addition, the local minima structures determined by the SCF procedure have been further characterized through harmonic frequency calculation. Another measure to ascertain the reliability of *ab initio* calculations is to analyze the properties of the wave function, such as bond orders, type of interaction between the nanotubes and the gas, density of states etc. These analyses have been performed using the NBO package of version 3.1 [23–25], Multiwfn software [26], and the GaussSum [27] package.

3 Result and Discussion

3.1 Geometric Surveys

The adsorption energy between the gas molecule and the nanotubes has been performed through the following steps.

First, the gas molecule and the nanotubes are optimized in isolation. Figure 1 shows the geometry of the optimized H_2SiCl_2 gas molecule.

The length (and diameter) of carbon and silicon carbide single-wall armchair (5,5) nanotubes are 22.89 Å (and 7.56 Å), 28.68 Å (and 8.27 Å), respectively. Such dimensions of the armchair nanotubes have previously been shown to describe the gas-nanotube interactions accurately [28–36]. Including the terminal hydrogens that are added to the nanotubes in order to reduce the boundary effects, each nanotube contains 200 atoms. The choice between armchair or zigzag type of nanotubes does not have a significant effect on the adsorption energy. Furthermore, we have also verified that increasing the length or diameter of the nanotube from the above-mentioned values has a minimal impact on the adsorption energy. Therefore, in order to minimize the computation time due to the size of the nanotubes, we have chosen the armchair (5,5) nanotube as the sensing material in this study.

Pristine silicon carbide nanotube has been used to model SiCGeNT nanotube. Briefly, one silicon atom has been replaced by a germanium atom, and the resulting structure is optimized by various DFT functional. Figure 2 shows a section of the CNT, SiCNT, and SiCGeNT nanotubes. It is evident from Fig. 2 that as the nature of the dopant atom, there are significant changes in various bond lengths. For example, in the pure CNT, the C – C bond length between two C atoms sharing two adjacent hexagonal rings is 1.43 Å. However, the corresponding bond (*i.e.*, C – Si bond) length subsequently increases to 1.78 Å in SiCNT, while

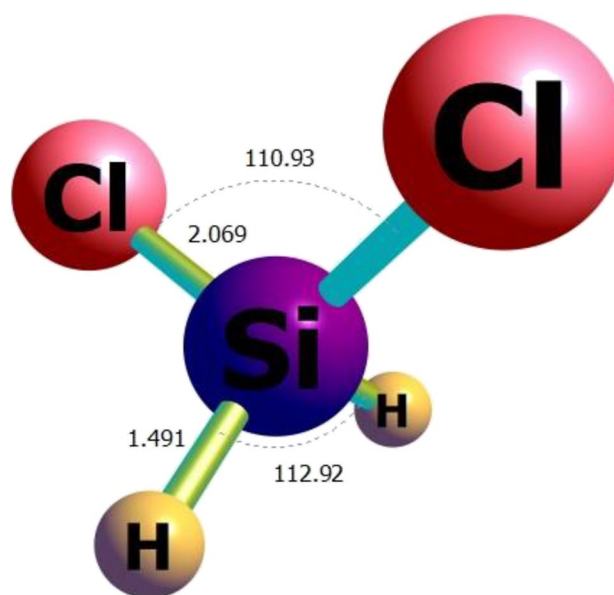


Fig. 1 The ground state structure of the H_2SiCl_2 molecule optimized using the B3LYP-D3 (GD3BJ)/6-311G(d) method. The bond length and bond angles are given in Å and degrees, respectively

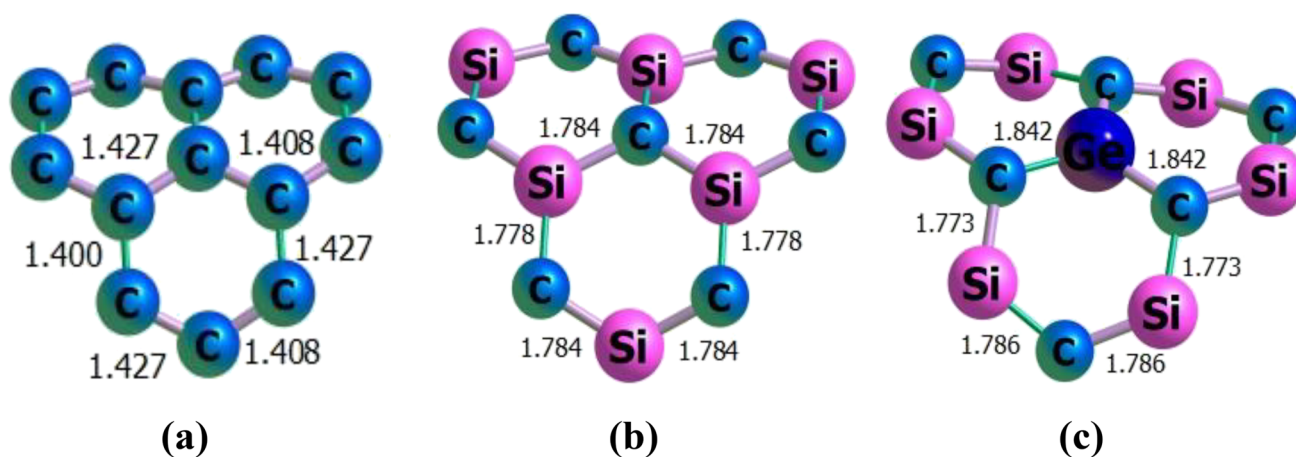


Fig. 2 Structural parameters (in Å) for (a) CNT, (b) SiCNT, and (c) SiCGeNT obtained at the B3LYP-D3 (GD3BJ)/6-311G(d) level

in SiCGeNT, it (the C – Ge bond) further increases to 1.84 Å. Consequently, these differences in the structural parameters affect adsorption energies between the nanotubes, as discussed later.

To calculate the adsorption energies on the three nanotubes, the gas molecule H_2SiCl_2 has been placed on the outer surface of each nanotube. To perform this task, we have placed the gas molecule at different distances and angles from the surface of the nanotube. As can be seen in Fig. 3, there are various positions (T_x) on the outer surface of the nanotubes on which gas can be placed. A chemically intuitive approach to obtain maximum interaction between the nanotubes and the overlying gas molecule is to place the chlorine head of H_2SiCl_2 on top of the above four positions, *i.e.*, T_1 to T_4 , on the surface of the nanotubes. Through this model, the distances between the gas and the nanotube are varied from 0.5 Å to 5 Å, resulting in 40 single-point *ab initio* energy

calculations for each T_x . To initiate these simulations, we have chosen the low-cost PBE0 functional. Geometry optimization calculations have been performed with the ωB97XD and M06-2X functionals to find the stable structures of nanotube- H_2SiCl_2 complexes for each T_x . Finally, we choose to further optimize the most stable nanotube- H_2SiCl_2 complexes among all adsorption positions (T_x) as obtained from the previous step with the more rigorous B3LYP-D3 (GD3BJ)/6-311G(d) method. It should be noted that all geometry optimization calculations are followed-up with harmonic frequency calculations to ascertain the true local minima. Figure 4 depicts the equilibrium structure of the most stable nanotube- H_2SiCl_2 complexes obtained by the B3LYP-D3 (GD3BJ) functional. It is evident from Fig. 4 that the T_2 site for CNT and T_3 site for doped SiCNT and SiCGeNT are the most favourable adsorption site for the Cl head of the gas to interact with the nanotubes.

Fig. 3 The four possible adsorption sites of the isolated nanotube. The gas molecule can be placed on top of the hexagonal ring (T_1); on top of the bond between two C/C and Si/C and Ge atoms (T_2); on top of a carbon atom (T_3); and on top of the silicon or germanium atom (T_4)

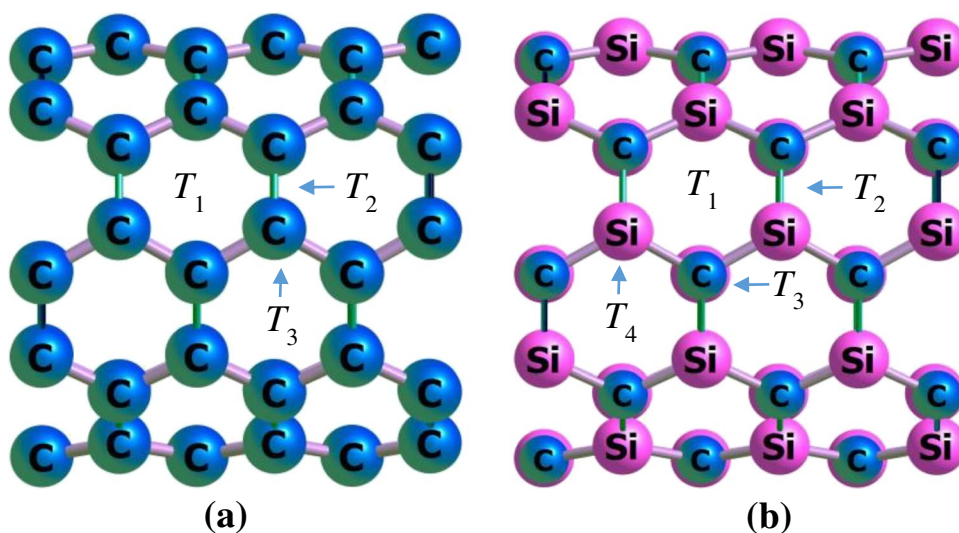
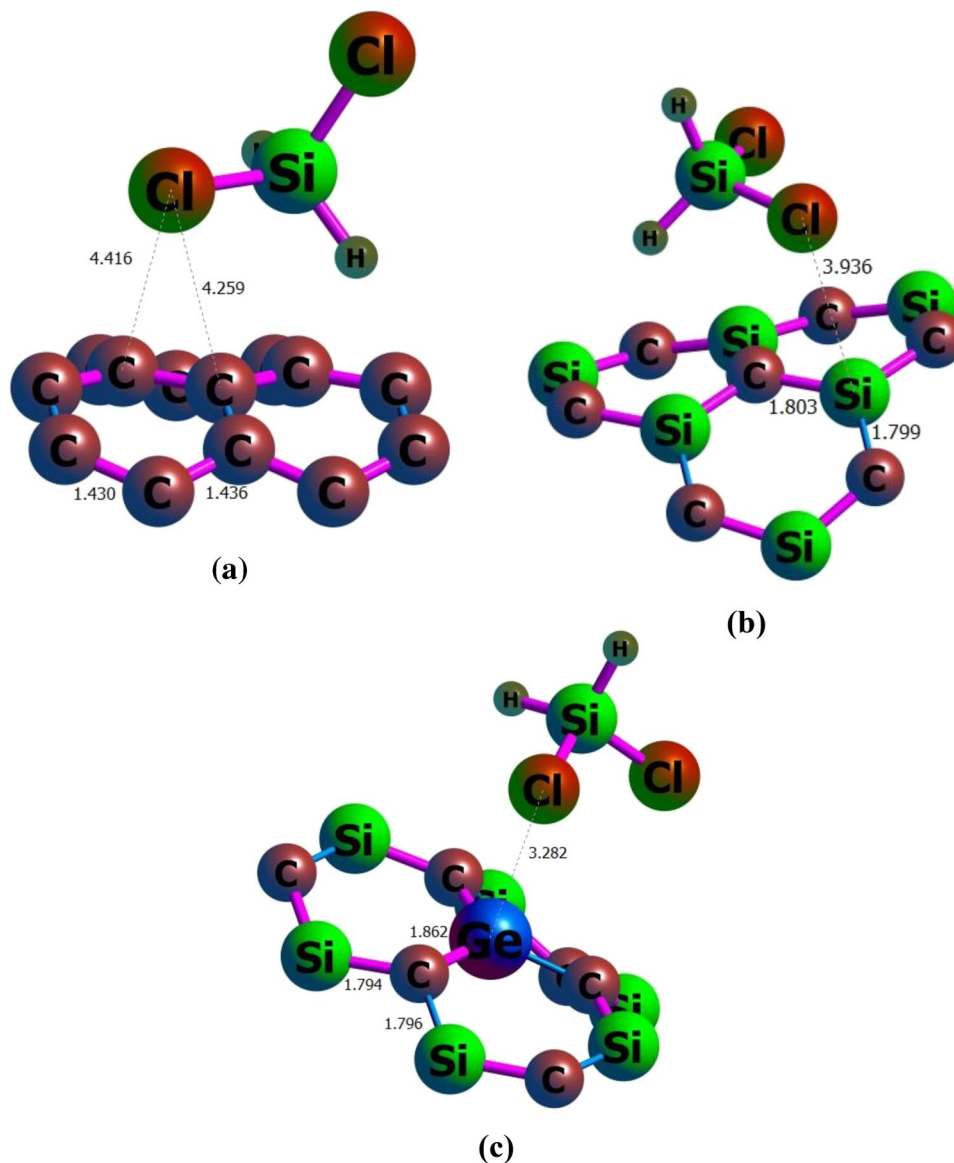


Fig. 4 The optimized structures of **a)** $\text{H}_2\text{SiCl}_2/\text{CNT}$, **b)** $\text{H}_2\text{SiCl}_2/\text{SiCNT}$, and **c)** $\text{H}_2\text{SiCl}_2/\text{SiC-GeNT}$ complex obtained by B3LYP-D3 (GD3BJ)/6-311G(d) method



The adsorption energy (E_{ads}) has been calculated as:

$$E_{\text{ads}} = E_{\text{tube/gas}} - E_{\text{tube}} - E_{\text{amino}} + \Delta E_{(\text{BSSE})} + \Delta E_{(\text{ZPE})} \quad (1)$$

where $E_{\text{tube/gas}}$ is the energy of the nanotube and gas complex, and E_{gas} and E_{tube} are the energies of the isolated gas and nanotube, respectively. Several additional energy corrections such as the basis set superposition error (BSSE), $\Delta E_{(\text{BSSE})}$ and zero-point energy (ZPE), $\Delta E_{(\text{ZPE})}$ correction has been taken into account to accurately determine the adsorption energies.

The numerical values of the adsorption energies calculated at the most stable nanotube- H_2SiCl_2 structure using four different functionals are reported in Table 1. Among all functionals, calculation by PBE0 functional amounts for the lowest adsorption energies, followed by the M06-2X

functional. On the other hand, the two functionals incorporating dispersion correction terms, *viz.* ωB97XD and B3LYP-D3 functionals have comparable E_{ads} values and are greater than those obtained by PBE0 and M06-2X functionals. In general, the doping of pure CNT, as well as the increase in the size of the dopant atom, increases the

Table 1 Adsorption energies (E_{ads}) of the H_2SiCl_2 molecule on CNT, SiCNT, and SiCGeNT using four different functionals. All values are in (eV)

Systems	PBE0	M06-2X	ωB97XD	B3LYP-D3
$\text{H}_2\text{SiCl}_2/\text{CNT}$	-0.075	-0.182	-0.269	-0.287
$\text{H}_2\text{SiCl}_2/\text{SiCNT}$	-0.088	-0.260	-0.311	-0.398
$\text{H}_2\text{SiCl}_2/\text{SiCGeNT}$	-0.367	-0.592	-0.629	-0.736

adsorption energy. The maximum E_{ads} found in this study amounts to -0.76 eV for SiCGeNT. The larger E_{ads} in SiC-GeNT may be related to the greater charge transfer from Ge to the Cl atom compared to the Si and C atoms.

3.2 Electronic Properties

One can determine many electronic properties of a molecule or a complex from the highest occupied molecular orbital (HOMO) and lowest unoccupied molecular orbitals (LUMO) obtained from standard DFT calculations. The ionization potential (IP) and electron affinity (EA) of a molecular system are related to the HOMO–LUMO energy gap (HLG) [37] according to Koopmans' [38] and Janak's [39] approximations, *i.e.*, $\epsilon_{\text{HOMO}} = -IP$ and $\epsilon_{\text{LUMO}} = -EA$. This energy gap changes during the gas adsorption process on the nanotube and, therefore, can produce a signal that activates the sensor circuit. Potentiometric and voltammetric sensors are also designed depending on whether the energy gap decreases or increases.

The electronic chemical potential (μ) and electronegativity (χ) are related to HOMO–LUMO energies as [40]:

$$-\chi = \mu \cong \frac{(\epsilon_{\text{HOMO}} + \epsilon_{\text{LUMO}})}{2} = \frac{1}{2}(IP + EA) \quad (2)$$

Similarly, the chemical hardness (η) [41] and electrophilicity (ω) [42] are defined in terms of HOMO–LUMO energies as,

$$\eta = \frac{1}{2}(IP - EA) \quad (3)$$

$$\omega = \frac{\mu^2}{2\eta} \quad (4)$$

The computed values of these electronic properties calculated at their equilibrium geometries are reported in Table 2. There is no significant change in the energy values of both HOMO and LUMOs for the transition from non-adsorbed to adsorbed state. These results signify that the gas–nanotube interactions are rather weak. This is true for both pristine and doped nanotubes. There is, however, a small increase in HLG for the adsorption of DCS on pristine CNT. In contrast, the doped nanotube shows a small decrease in HLG values

upon gas adsorption. It is interesting to note that the HLG in CNT is much smaller (0.67 eV) either in the adsorbed or non-adsorbed state in comparison to the SiCNT or SiCGeNTs (3.32 – 3.35 eV). The HOMO–LUMO energy gaps can also be visually examined from the corresponding density of states (DOS) diagrams, as pictured in Fig. 5.

Naturally, molecules with large HLG will have high values of η , whereas those with low HLG have low η values, as can be seen in Table 2. The chemical hardness of the doped nanotubes is much greater than the pristine CNT, which reduces slightly after the adsorption of DCS onto its surface. On the other hand, the chemical potential for each nanotube in both adsorbed and non-adsorbed states is almost constant, hovering around a value between -3.6 eV to -3.7 eV. Finally, the electrophilicity ω index is also reduced due to adsorption. Analogous to η values, ω values are much greater for both SiCNT and SiCGeNT than the pristine CNT.

Another factor to consider in sensor design is Recovery time (RT). This means that the absorption power of the sensor surface is directly related to the absorption energy and is expressed as follows [43]:

$$RT = \nu_o^{-1} \exp\left(\frac{E_{\text{ads}}}{kT}\right) \quad (5)$$

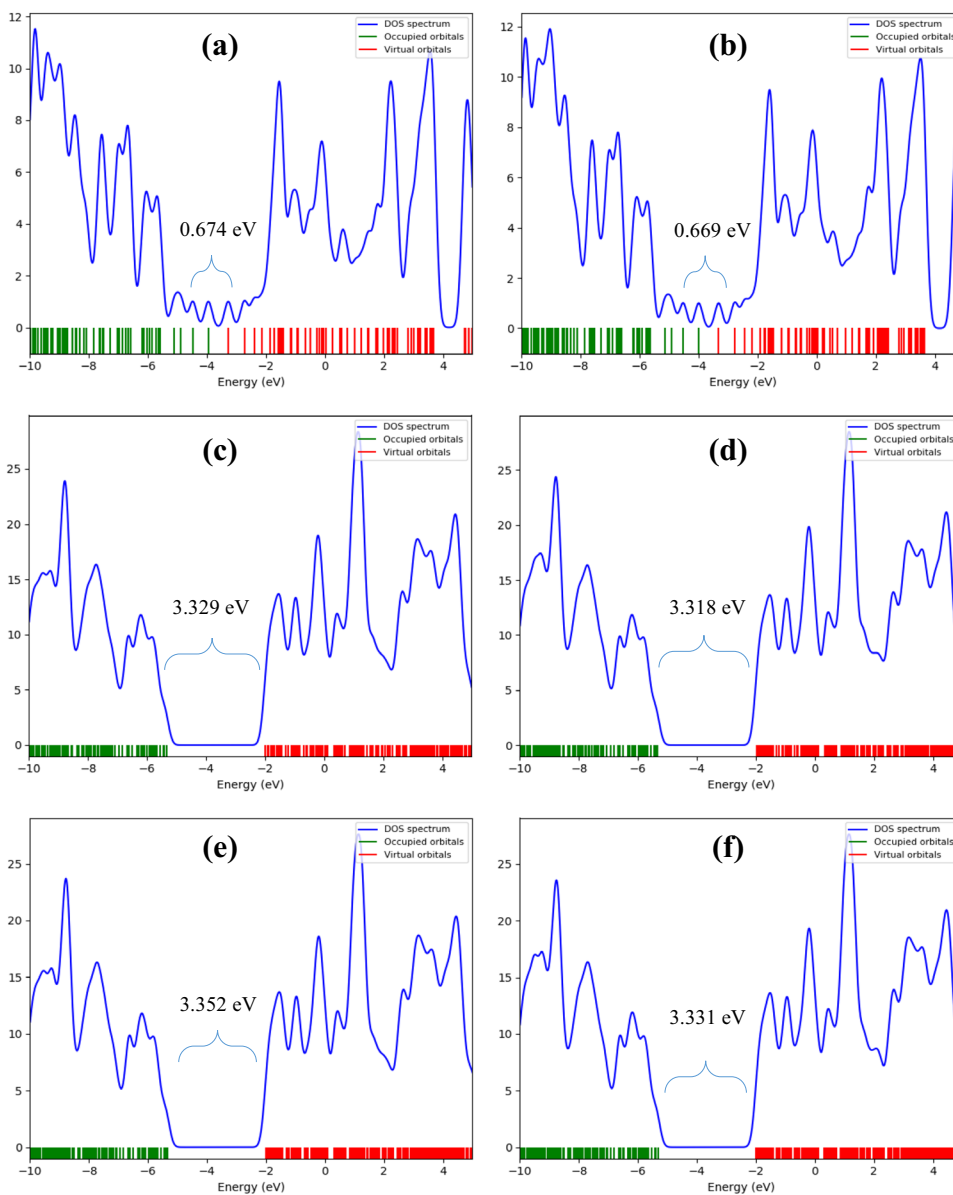
in this formula, k denotes the Boltzmann constant, T is referred to the temperature, and ν_o signifies the attempt frequency. According to the above relation, because the adsorption energy of silicon carbide nanotubes doped with germanium element provides the most adsorption energy among the others, thus its recovery time is better than the others. From the point of view of the adsorption mechanism for designing a sensor, it has been experimentally proven that there is a relationship between the dependence of the sensing mechanism and the change in the resistance of the sensor due to the charge transfer between the sensor and the absorbate material. Therefore, if a change is made in the level of the sensor and disturbs its electronic properties, then some parameters such as electrical conductivity (σ) and resistance (R) change, the following relationships can be used to explain them,

$$\sigma = AT^{3/2} \exp\left(\frac{E_{\text{HLG}}}{2kT}\right) \quad (6)$$

Table 2 Energy of the HOMO (ϵ_{H}) and LUMO (ϵ_{L}); HOMO–LUMO energy gap (HLG); chemical potential (μ); chemical hardness (η); and electrophilicity (ω) obtained at B3LYP-D3 (GD3BJ)/6-311G (d) level of theory. All values are in eV

Systems	ϵ_{H}	ϵ_{L}	HLG	μ	η	ω
CNT	-3.950	-3.276	0.674	-3.613	0.337	2.200
SiCNT	-5.340	-2.011	3.329	-3.675	1.665	11.243
SiCGeNT	-5.344	-1.992	3.352	-3.668	1.676	11.275
H ₂ SiCl ₂ /CNT	-3.997	-3.328	0.669	-3.662	0.335	2.244
H ₂ SiCl ₂ /SiCNT	-5.334	-2.016	3.318	-3.675	1.659	11.203
H ₂ SiCl ₂ /SiCGeNT	-5.321	-1.990	3.331	-3.655	1.665	11.125

Fig. 5 Density of state maps for **a)** CNT, **b)** H₂SiCl₂/CNT, **c)** SiCNT, **d)** H₂SiCl₂/SiCNT, **e)** SiCGeNT, **f)** H₂SiCl₂/SiCGeNT. Data obtained using the B3LYP-D3 (GD3BJ)/6-311G(d) method



where A is a constant, k is the Boltzmann constant and, T is temperature. The sensing response (SR) is considered as follows [44],

$$SR = \frac{|R_2 - R_1|}{R_1} \tag{7}$$

In the above relation, R1 is related to the absorber resistance and R2 is related to the sensor/gas resistance. It should be noted that SR and σ are related according to the following relation [45]:

$$SR = \left| \frac{\sigma_1}{\sigma_2} \right| - 1 = \exp\left(\frac{\Delta E_{HLG}}{2kT}\right) - 1 \tag{8}$$

where σ_1 and σ_2 denote electrical conductivity of pure sensor and sensor/gas cluster, respectively. Given the above relationships, it is very clear that germanium-doped silicon carbide nanotubes are a suitable option for fabrication and

Table 3 Values of Mulliken and Mayer bond order and Wiberg bond index calculated by B3LYP-D3/6-311G(d) method

Systems	X ^aY ^b	Mulliken	Mayer	Wiberg
H ₂ SiCl ₂ /CNT	Cl.....C	0.044	0.077	0.074
H ₂ SiCl ₂ /SiCNT	Cl.....Si	0.079	0.116	0.157
H ₂ SiCl ₂ /SiCGeNT	Cl....Ge	0.122	0.159	0.257

^aX atom belongs to H₂SiCl₂

^bY atom belongs to nanotube

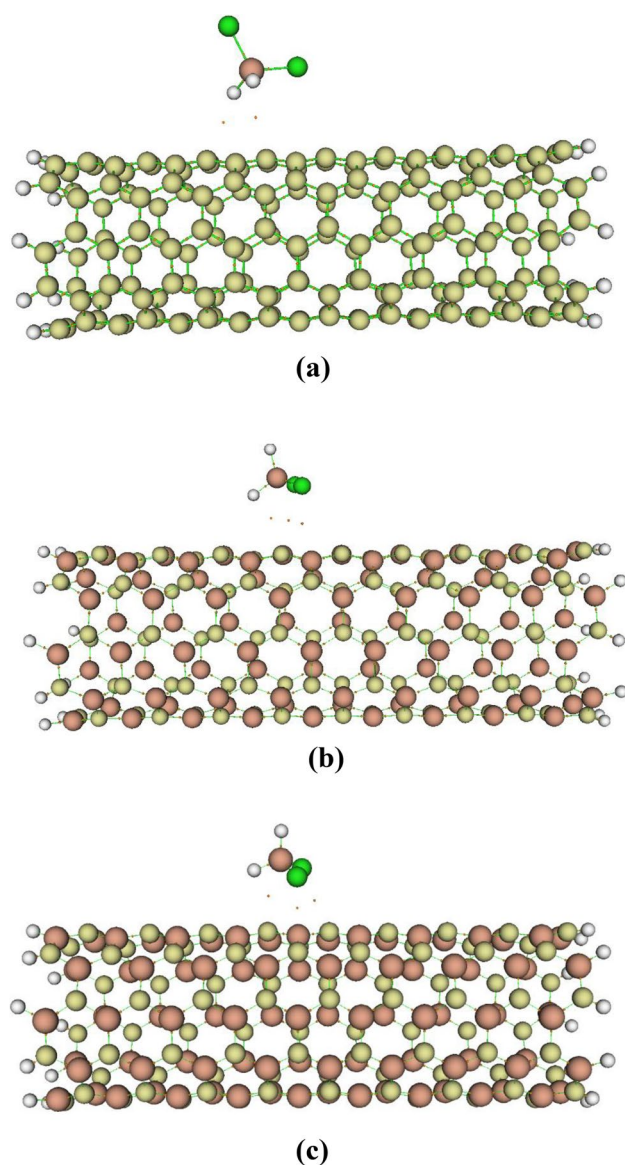


Fig. 6 The bond critical points (BCP) graphs for the **a**) $\text{H}_2\text{SiCl}_2/\text{CNT}$, **b**) $\text{H}_2\text{SiCl}_2/\text{SiCNT}$, **c**) and $\text{H}_2\text{SiCl}_2/\text{SiCGeNT}$ systems. The orange dots represent the BCPs

Table 4 QTAIM topological parameters for electron density $\rho(\mathbf{r})$, Laplacian of electron density $\nabla^2\rho(\mathbf{r})$, kinetic electron density $G(\mathbf{r})$, potential electron density $V(\mathbf{r})$, and the ratio of $G(\mathbf{r})/V(\mathbf{r})$ at the BCPs

Systems	Bond	$\rho(\mathbf{r})$	$\nabla^2\rho(\mathbf{r})$	$G(\mathbf{r})$	$V(\mathbf{r})$	$G(\mathbf{r})/V(\mathbf{r})$
$\text{H}_2\text{SiCl}_2/\text{CNT}$	Cl.....C	0.0033	0.0101	0.0019	-0.0014	1.4276
	C.....C	0.0038	0.0111	0.0022	-0.0017	1.3328
$\text{H}_2\text{SiCl}_2/\text{SiCNT}$	Cl....Si	0.0048	0.0126	0.0025	-0.0019	1.3322
	C.....Si	0.0043	0.0112	0.0023	-0.0017	1.3237
$\text{H}_2\text{SiCl}_2/\text{SiCGeNT}$	Cl....Ge	0.0042	0.0113	0.0022	-0.0017	1.3410
	Cl.....Si	0.0110	0.0281	0.0062	-0.0054	1.1498
	C.....Ge	0.0047	0.0122	0.0025	-0.0019	1.2824

design of related sensors for adsorption of H_2SiCl_2 molecule due to their higher sensitivity.

3.3 Natural Bond Orbital (NBO) Analysis

The bond order between the Cl head of DCS and the nanotube has been evaluated by natural bond orbital (NBO) analysis. There are several methods through which bond order between two atoms can be calculated. Among them, the Mulliken method [46], Meyer method [47–49], and Weiberg method [50, 51] are studied here. The calculated bond order between the Cl atom of DCS and C atom (CNT), Si atom (SiCNT), and Ge atom (SiCGeNT) are reported in Table 3. It is clear from Table 3 that as the size of the dopant atom increases, there is a corresponding increase in the bond order. For example, the Wiberg bond index (WBI) is 0.07 for pristine CNT, indicating that the interaction between the Cl atom and C atom is very weak and can be considered as van der Waals interaction. On the other hand, the Cl-Ge and Cl-Si interaction are comparatively stronger. These results are fully consistent with the observations detailed in the previous two subsections, *i.e.*, the Cl-Ge interaction is stronger due to greater charge transfer between them.

3.4 Quantum Theory of Atoms In Molecules (QTAIM) Analysis

Bader's QTAIM analysis [52, 53] can be used to interpret many types of intermolecular interactions present in a molecule. Electron density $\rho(\mathbf{r})$ is a key quantity in this analysis from which a set of parameters are obtained. From the topological analysis of electron densities around a bond, a bond critical point (BCP) can be defined as a saddle point in electron density ($\nabla^2\rho(\mathbf{r})=0$) that has maximum electron density in two perpendicular directions and minimum in the other [54]. The BCPs of the $\text{H}_2\text{SiCl}_2/\text{CNT}$, $\text{H}_2\text{SiCl}_2/\text{SiCNT}$ and $\text{H}_2\text{SiCl}_2/\text{SiCGeNT}$ complexes at their optimized geometry

of the H_2SiCl_2 clusters with CNT, SiCNT, and SiCGeNT. All values have been calculated using the B3LYP-D3 (GD3BJ)/6-311G(d) method

are illustrated in Fig. 6. It is clear from this figure that all nanotube – H_2SiCl_2 interactions are relatively weak.

For intermolecular interactions of the covalent type, the electron density in BCP are large ($\rho(\mathbf{r}) > 0.2$ a.u.) and the Laplacian of electron density values are less than zero ($\nabla^2\rho(\mathbf{r}) < 0$). Conversely, if $\rho(\mathbf{r})$ is less than 0.1 a.u. and $\nabla^2\rho(\mathbf{r})$ is positive, then the interactions can be considered as closed-shell type, indicating a hydrogen bond, weak van der Waals interactions, or a presence of an ionic bond [55]. From Table 4, we can see that the electron density values are always smaller than 0.1 a.u. for Cl—X interactions (X \equiv C, Si or Ge). Moreover, the Laplacian of electron density values is also positive. These results indicate that Cl—X interactions are of non-covalent type.

The Lagrangian kinetic energy density $G(\mathbf{r})$ and potential energy density $V(\mathbf{r})$ can be related to the Laplacian according to the virial theorem [56]:

$$\frac{1}{4}\nabla^2\rho(r) = 2G(r) + V(r) \quad (9)$$

Their ratio can also be a good indicator of bonding characteristics. For a covalent bond, $G(\mathbf{r})/|V(\mathbf{r})|$ ratio is less than 0.5 and for non-covalent interaction $G(\mathbf{r})/|V(\mathbf{r})| > 1$. The numerical values of these ratios are listed in Table 4. These values further emphasize the existence of prominent non-covalent interaction between Cl atom and X atom (X \equiv C, Si or Ge) in all H_2SiCl_2 – nanotube complexes studied in this work.

4 Conclusion

In this work, we have evaluated the feasibility of gaseous dichlorosilane (DCS, H_2SiCl_2) molecule adsorption on pristine carbon nanotubes (CNT), silicon carbide nanotube (SiCNT), and on Ge atom doped silicon carbide nanotube (SiCGeNT). We have employed a dispersion corrected B3LYP-D3 (GD3BJ) functional with a 6-311G(d) basis set to determine the most crucial electronic properties for gas-nanotube interactions, such as the adsorption energy, HOMO and LUMO energies, bond orders, QTAIM analysis etc. The PBE0, ω B97XD and M06-2X functionals have also been employed to show that the inclusion of dispersion term within the functional is pivotal for accurate determination of the adsorption energies. Full dimensional geometry optimization calculations show that the adsorption of DCS primarily occurs through one of the Cl atoms of H_2SiCl_2 interacting directly on top of the C atom for pristine CNT and Si and Ge atoms for doped CNTs. We find that as the size of the dopant atom increases, there is an incremental increase in the adsorption energy, with SiCGeNT releasing maximum energy (≈ 0.74 eV). From HOMO–LUMO energies, NBO,

and QTAIM analyses, we find that the interaction between the gas and nanotubes is weak and, therefore, can be categorized as physisorption.

Acknowledgements HYA thanks the Solid-State Theory Group, Physics Department, Università degli Studi di Milano, Milan, Italy, for providing computational facilities. SB and GB acknowledge the support of the European Regional Development Fund and the Republic of Cyprus through the Research Innovation Foundation (Cy-Tera project under the grant NEA YPODOMH/STPATH/0308/31, and NANO²LAB project under the grant INFRASTRUCTURES/1216/0070).

Author Contribution Mohsen Doust Mohammadi: Writing – original draft, Formal analysis. Hewa Y. Abdullah: Supervision, Investigation, Project administration. Somnath Bhowmick: Conceptualization, Validation. George Biskos: Resources, Visualization.

Data Availability Not applicable.

Declarations

Ethics Approval and Consent to Participate All authors agree.

Consent for Publication All authors agree.

Conflicts of Interest The authors declare that they have no known competing financial interests or personal relationships that could have appeared to influence the work reported in this paper.

Research Involving Human Participants and/or Animals Not applicable.

Informed Consent All authors agree.

References

1. Kaushik A, Kumar R, Jayant RD, Nair M (2015) Nanostructured gas sensors for health care: An overview. *J Personalized Nanomed* 1:10
2. Dallinger D, Kappe CO (2017) Lab-scale production of anhydrous diazomethane using membrane separation technology. *Nat Protoc* 12:2138–2147
3. Ishii A, Yamamoto M, Asano H, Fujiwara K (2008) DFT calculation for adatom adsorption on graphene sheet as a prototype of carbon nanotube functionalization, *Journal of Physics: Conference Series*, IOP Publishing, pp 052087
4. DoustMohammadi M, Abdullah HY (2020) The adsorption of chlorofluoromethane on pristine, and Al- and Ga-doped boron nitride nanosheets: a DFT, NBO, and QTAIM study. *J Mol Model* 26:287
5. Mohammadi MD, Abdullah HY, Suvitha A (2021) The adsorption of 1-chloro-1, 2, 2, 2-tetrafluoroethane onto the pristine, Al-, and Ga-doped boron nitride nanosheet. *Iran J Sci Technol Transac A Sci* 45:1287–1300
6. Hurst J (2014) Boron nitride nanotubes, silicon carbide nanotubes, and carbon nanotubes—a comparison of properties and applications, nanotube superfiber materials. Elsevier, pp 267–287
7. Vorotyntsev V, Mochalov G, Kolotilova M, Volkova E (2006) Gas-chromatographic and mass-spectrometric determination of impurity hydrocarbons in organochlorine compounds and dichlorosilane. *J Anal Chem* 61:883–888

8. Seyferth D, Prud'homme C, Wiseman GH (1983) Cyclic polysiloxanes from the hydrolysis of dichlorosilane. *Inorg Chem* 22:2163–2167
9. Walch SP, Dateo CE (2001) Thermal decomposition pathways and rates for silane, chlorosilane, dichlorosilane, and trichlorosilane. *J Phys Chem A* 105:2015–2022
10. Mohammadi MD, Abdullah HY, Biskos G, Bhowmick S (2021) Effect of Al- and Ga-doping on the adsorption of H_2SiCl_2 onto the outer surface of boron nitride nanotube: a DFT study. *C R Chim* 24:291–304
11. Mohammadi MD, Abdullah HY, Louis H, Mathias GE (2022) 2D Boron Nitride Material as a sensor for H_2SiCl_2 . *Comput Theor Chem* 1213:113742
12. Grimme S, Ehrlich S, Goerigk L (2011) Effect of the damping function in dispersion corrected density functional theory. *J Comput Chem* 32:1456–1465
13. Goerigk L, Grimme S (2011) A thorough benchmark of density functional methods for general main group thermochemistry, kinetics, and noncovalent interactions. *Phys Chem Chem Phys* 13:6670–6688
14. Mardirossian N, Head-Gordon M (2017) Thirty years of density functional theory in computational chemistry: an overview and extensive assessment of 200 density functionals. *Mol Phys* 115:2315–2372
15. Brakestad A, Jensen SR, Wind P, D'Alessandro M, Genovese L, Hopmann KH, Frediani L (2020) Static polarizabilities at the basis set limit: A benchmark of 124 species. *J Chem Theory Comput* 16:4874–4882
16. Mitra H, Roy TK (2020) Comprehensive Benchmark results for the accuracy of basis sets for anharmonic molecular vibrations. *J Phys Chem A* 124:9203–9221
17. Goerigk L, Hansen A, Bauer C, Ehrlich S, Najibi A, Grimme S (2017) A look at the density functional theory zoo with the advanced GMTKN55 database for general main group thermochemistry, kinetics and noncovalent interactions. *Phys Chem Chem Phys* 19:32184–32215
18. Perdew JP, Ernzerhof M, Burke K (1996) Rationale for mixing exact exchange with density functional approximations. *J Chem Phys* 105:9982–9985
19. Adamo C, Barone V (1999) Toward reliable density functional methods without adjustable parameters: The PBE0 model. *J Chem Phys* 110:6158–6170
20. Zhao Y, Truhlar DG (2008) The M06 suite of density functionals for main group thermochemistry, thermochemical kinetics, noncovalent interactions, excited states, and transition elements: two new functionals and systematic testing of four M06-class functionals and 12 other functionals. *Theoret Chem Acc* 120:215–241
21. Zhao Y, Truhlar DG (2006) Density functional for spectroscopy: no long-range self-interaction error, good performance for Rydberg and charge-transfer states, and better performance on average than B3LYP for ground states. *J Phys Chem A* 110:13126–13130
22. Frisch MJ, Trucks GW, Schlegel HB, Scuseria GE, Robb MA, Cheeseman JR, Scalmani G, Barone V, Petersson GA, Nakatsuji H, Li X, Caricato M, Marenich AV, Bloino J, Janesko BG, Gomperts R, Mennucci B, Hratchian HP, Ortiz JV, Izmaylov AF, Sonnenberg JL, Williams, Ding F, Lipparini F, Egidi F, Goings J, Peng B, Petrone A, Henderson T, Ranasinghe D, Zakrzewski VG, Gao J, Rega N, Zheng G, Liang W, Hada M, Ehara M, Toyota K, Fukuda R, Hasegawa J, Ishida M, Nakajima T, Honda Y, Kitao O, Nakai H, Vreven T, Throssell K, Montgomery Jr JA, Peralta JE, Ogliaro F, Bearpark MJ, Heyd JJ, Brothers EN, Kudin KN, Staroverov VN, Keith TA, Kobayashi R, Normand J, Raghavachari K, Rendell AP, Burant JC, Iyengar SS, Tomasi J, Cossi M, Millam JM, Klene M, Adamo C, Cammi R, Ochterski JW, Martin RL, Morokuma K, Farkas O, Foresman JB, Fox DJ (2016) Gaussian 16 Rev. C.01, Wallingford, CT
23. Foster AJ, Weinhold F (1980) Natural hybrid orbitals. *J Am Chem Soc* 102:7211–7218
24. Reed AE, Weinhold F (1983) Natural bond orbital analysis of near-Hartree–Fock water dimer. *J Chem Phys* 78:4066–4073
25. Carpenter J, Weinhold F (1988) Analysis of the geometry of the hydroxymethyl radical by the “different hybrids for different spins” natural bond orbital procedure. *J Mol Struct (Theochem)* 169:41–62
26. Lu T, Chen F (2012) Multiwfn: a multifunctional wavefunction analyzer. *J Comput Chem* 33:580–592
27. O'boyle NM, Tenderholt AL, Langner KM (2008) CcLib: a library for package-independent computational chemistry algorithms. *J Comput Chem* 29:839–845
28. Mohammadi MD, Hamzehloo M (2018) The adsorption of bromomethane onto the exterior surface of aluminum nitride, boron nitride, carbon, and silicon carbide nanotubes: a PBC-DFT, NBO, and QTAIM study. *Comput Theor Chem* 1144:26–37
29. DoustMohammadi M, Abdullah HY (2020) The adsorption of chlorofluoromethane on pristine, Al-, Ga-, P-, and As-doped boron nitride nanotubes: a PBC-DFT, NBO, and QTAIM study. *ChemistrySelect* 5:12115–12124
30. Mohammadi MD, Salih IH, Abdullah HY (2020) The adsorption of chlorofluoromethane on pristine and Ge-doped silicon carbide nanotube: a PBC-DFT, NBO, and QTAIM study. *Mol Simul* 46:1405–1416
31. DoustMohammadi M, Abdullah HY (2021) The adsorption of bromochlorodifluoromethane on pristine and Ge-doped silicon carbide nanotube: a PBC-DFT, NBO, and QTAIM study. *Struct Chem* 32:481–494
32. Mohammadi MD, Abdullah HY (2021) The adsorption of bromochlorodifluoromethane on pristine, Al, Ga, P, and As-doped boron nitride nanotubes: a study involving PBC-DFT, NBO analysis, and QTAIM. *Comput Theor Chem* 1193:113047
33. Mohammadi MD, Abdullah HY (2021) Vinyl chloride adsorption onto the surface of pristine, Al-, and Ga-doped boron nitride nanotube: A DFT study. *Solid State Commun* 337:114440
34. Mohammadi MD, Abdullah HY (2021) DFT Study for Adsorbing of Bromine Monochloride onto BNNT (5, 5), BNNT (7, 0), BC 2 NNT (5, 5), and BC 2 NNT (7, 0). *J Comput Biophys Chem* 20:765–783
35. Mohammadi MD, Abdullah HY, Biskos G, Bhowmick S (2021) Enhancing the absorption of 1-chloro-1, 2, 2-tetrafluoroethane on carbon nanotubes: an *ab initio* study. *Bull Mater Sci* 44:198
36. DoustMohammadi M, Abdullah HY (2022) Weak intermolecular interactions of cysteine on BNNT, BNAINT and BC2NNT: a DFT investigation. *Bull Mater Sci* 45:33
37. Bredas J-L (2014) Mind the gap! *Mater Horiz* 1:17–19
38. Koopmans T (1934) Über die Zuordnung von Wellenfunktionen und Eigenwerten zu den einzelnen Elektronen eines Atoms. *Physica* 1:104–113
39. Janak J (1978) Proof that $\partial \epsilon_n / \partial n_i = \epsilon_i$ in density-functional theory. *Phys Rev B* 18:7165
40. Parr RG, Donnelly RA, Levy M, Palke WE (1978) Electronegativity: the density functional viewpoint. *J Chem Phys* 68:3801–3807
41. Parr RG, Pearson RG (1983) Absolute hardness: companion parameter to absolute electronegativity. *J Am Chem Soc* 105:7512–7516
42. Levy M (1982) Electron densities in search of Hamiltonians. *Phys Rev A* 26:1200
43. Baei MT, Peyghan AA, Bagheri Z (2012) A computational study of AlN nanotube as an oxygen detector. *Chin Chem Lett* 23:965–968

44. Yamazoe N, Shimano K (2009) New perspectives of gas sensor technology. *Sens Actuators, B Chem* 138:100–107
45. Hamprecht FA, Cohen AJ, Tozer DJ, Handy NC (1998) Development and assessment of new exchange-correlation functionals. *J Chem Phys* 109:6264–6271
46. Mulliken RS (1955) Electronic population analysis on LCAO–MO molecular wave functions I. *J Chem Phys* 23:1833–1840
47. Mayer I (1983) Charge, bond order and valence in the *Ab initio* SCF theory. *Chem Phys Lett* 97:270–274
48. Mayer I (2012) Improved definition of bond orders for correlated wave functions. *Chem Phys Lett* 544:83–86
49. Bridgeman AJ, Cavigliasso G, Ireland LR, Rothery J (2001) The Mayer bond order as a tool in inorganic chemistry. *J Chem Soc Dalton Trans* 2095–2108
50. Wiberg KB (1968) Application of the pople-santry-segal CNDO method to the cyclopropylcarbanyl and cyclobutyl cation and to bicyclobutane. *Tetrahedron* 24:1083–1096
51. Sizova OV, Skripnikov LV, Sokolov AY (2008) Symmetry decomposition of quantum chemical bond orders. *J Mol Struct (Theor Chem)* 870:1–9
52. Bader RF (1985) *Atoms in molecules*. *Acc Chem Res* 18:9–15
53. Bader R (1990) *A quantum theory*. Clarendon, Oxford
54. Bader RFW, Popelier PLA, Keith TA (1994) Theoretical definition of a functional group and the molecular orbital paradigm. *Angew Chem Int Ed Engl* 33:620–631
55. Matta CF (2006) Hydrogen–hydrogen bonding: the non-electrostatic limit of closed-shell interaction between two hydro, *Hydrogen Bonding—New Insights*, Springer, pp 337–375
56. Grabowski SJ (2012) QTAIM characteristics of halogen bond and related interactions. *J Phys Chem A* 116:1838–1845

Publisher's Note Springer Nature remains neutral with regard to jurisdictional claims in published maps and institutional affiliations.